Nonlinear Dyn (2013) 73:737–749
DOI 10.1007/s11071-013-0827-6

ORIGINAL PAPER

Stability and Hopf bifurcation in an inverted pendulum with delayed feedback control

Rui Yang · Yahong Peng · Yongli Song

Received: 27 May 2012 / Accepted: 9 February 2013 / Published online: 20 February 2013

Abstract In this paper, we investigate the dynamics of the inverted pendulum with delayed feedback control. The existence and stability of multiple equilibria depending on the control strengths are studied. Taking the time delay of the control terms as a parameter, periodic oscillations induced by delay are found. By using the method of multiple scales, the effect of the control gains and the relative mass of the pendulum on the stability and direction of Hopf bifurcations are discussed. Numerical simulations are employed to illustrate the obtained theoretical results.

Keywords Inverted pendulum · Discrete delay · Method of multiple scales · Hopf bifurcation

1 Introduction

In the field of control theory, research on the inverted pendulum have implications for a great many typical problems such as nonlinearity, robustness, and stabilization. Many control systems have been designed for stabilizing and controlling the amplitude of a single inverted pendulum that is either fixed to the ground or on a cart that moves on a rail. The study of the single inverted pendulum originated from the rocket booster, then stimulated by the biped robot there are extensive discussions on the multiple inverted pendulums. The research methods and technologies arising from the model of the inverted pendulum(s) attribute to the applications to both biological and mechanical balancing tasks, such as how to avoid falling in the elderly while walking, vertical launch of a rocket, control the motion of the robot, and space docking. Also, by means of the rich properties the inverted pendulum provides, the model plays an important role in detecting abilities of new control methods on dealing with nonlinearity and instability. The control process aims at better performance of stabilizing the inverted pendulum at the balancing position without exaggerated robustness and oscillation. See [1–7] for the dynamical research of the inverted pendulum and its applications.

Typically, when the friction between the cart and the track together with the friction between the pendulum and the pivot are neglected, the dynamics of the inverted pendulum fixed through a pivot on a cart that moves on a rail are governed by the following equations [8] using Hamilton's principle (see Fig. 1):

$$\begin{cases} (m+M)\ddot{x}(t) + m\frac{\ell}{2}\ddot{\theta}(t)\cos\theta(t) - m\frac{\ell}{2}\dot{\theta}^2(t)\sin\theta(t) \\ \quad = F(t), \\ m\frac{\ell}{2}\ddot{x}(t)\cos\theta(t) + \frac{4}{3}m(\frac{\ell}{2})^2\ddot{\theta}(t) - mg\frac{\ell}{2}\sin\theta(t) = 0. \end{cases}$$

See Table 1 for the physical meaning of the parameters.

R. Yang · Y. Song (✉)
Department of Mathematics, Tongji University, Shanghai 200092, China
e-mail: 05143@tongji.edu.cn

Y. Peng
Department of Applied Mathematics, Donghua University, Shanghai 200051, China

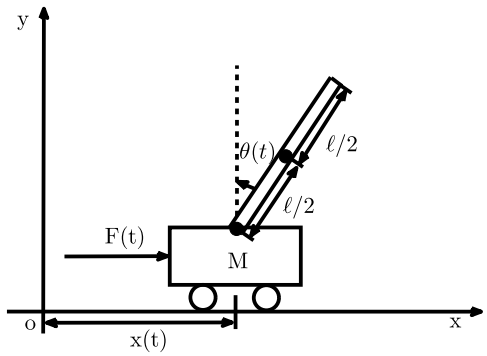

Fig. 1 The corresponding model of the inverted pendulum on a cart

Table 1 Parameters for the neglected friction model

Parameters	Description
m	Mass of the pendulum
M	Mass of the cart
$x(t)$	Displacement of the center of mass of the cart
ℓ	Length of the pendulum
$F(t)$	Horizontal control force applied to the cart
$\theta(t)$	Rotation angle of the pendulum away from the top vertical position ($\theta(t) \in [0, 2\pi]$)

Generally, the control action will take effect only after some fixed time and the linear control force depending on the rotation angle θ and its velocity $\dot{\theta}$ are often used in the literature [9, 10] as follows:

$$F(t) = a\theta(t-\tau) + b\dot{\theta}(t-\tau),$$

where $a, b > 0$ are the control gains. Eliminating $\ddot{x}(t)$ and then rescaling F and the time t by $(M+m)g$ and $\sqrt{3g/2\ell}$, respectively, we have the following second-order differential equation for the rotation angular:

$$\left(1 - \frac{3\rho}{4}\cos^2\theta(t)\right)\ddot{\theta}(t) + \frac{3\rho}{8}\dot{\theta}^2(t)\sin\big(2\theta(t)\big) - \sin\theta(t) + \big(a\theta(t-\tau) + b\dot{\theta}(t-\tau)\big)\cos\theta(t) = 0, \tag{1}$$

where $\rho = \frac{m}{(m+M)} < 1$ is the relative mass of the pendulum.

The existence of time delay makes the system become an infinite dimensional dynamics, which leads to more abundant dynamics, but substantially complicates the theoretical analysis. The dynamics of the inverted pendulum with delayed feedback control have been studied by several authors. A mechanical model of a digital balancing system is constructed and its stability analysis is presented considering experimental problems like backlash and sampling delay in [12], and also the existence and stability of periodic solutions are checked analytically in [13]. Stépán and Kollár [14] construct the stability chart in the space of the control parameters and the analytical results are correlated with the experimental observations. Atay [15] presents sharp results on how to choose the feedback parameters of the inverted pendulum with position feedback to obtain asymptotic stability. Landry et al. [16] consider an inverted pendulum attached to a cart with the delayed control force, which not only depends on the voltage in the motor driving the cart and the resistance, but also counters the electromotive force. They show that for values of the delay below a critical delay, the system remains stable and the system undergoes a supercritical Hopf bifurcation at the critical delay. In [8, 17, 18], there are three kinds of friction taken into consideration: simple viscous friction and two stick slip frictions. Cabrera and Milton [19] present some experimental observations reproduced by a model of an inverted pendulum with time delayed feedback. Especially, we would like to mention the works of Sieber and Krauskopf [9, 10, 20], which are most directly related to our work. In [9], the linear stability of system (1) at the origin has been analyzed. Also, Sieber and Krauskopf show there is a codimension-three bifurcation point in (1), and then by computing and analyzing a reduced three-dimensional center manifold they find the stable small-amplitude solutions outside the region of the linear stability of the pendulum. In [10], Sieber and Krauskopf show that system (1) may exhibit small chaotic motion about the upside-down position and find the complex motion near the triple-zero eigenvalue singularity. In addition, we would like to mention that in the absence of feedback control, the stabilization of inverted pendulum can be achieved by using the high-frequency excitation. This is also a famous problem and has been extensively studied in the field of mechanics and applied mathematics. We refer the interested readers to a detailed review due to Ibrahim [11] for more information.

The ultimate goal of controlling the cart-pendulum system is to turn the unstable system into a stable one through the proper ways of control. Once the model has been set up, we can find the balancing position by

adjusting the values of parameters. As we all know, without any control, the pendulum can stay stable in the downright position while unstable in the upright position. Here, we focus on when and where the pendulum can stay balancing or generate low amplitude oscillation with the horizontal linear feedback control, which can be explored through the linear stability analysis and Hopf bifurcation analysis. Once the equilibria found, the aim to stabilize the pendulum in the equilibrium position can be achieved by modulating the values of the parameters and the time delay. The low amplitude oscillation corresponds to the periodic solution bifurcating from the equilibria. Except for the zero solution, the cart-pendulum system exists multiple nonzero equilibria depending on the value of the control gain a in system (1). The main purpose of this paper is to investigate the stability of nonzero equilibria and figure out how the direction and stability of Hopf bifurcations induced by delay depend on the relative mass and the control gains.

This paper is organized as follows. Starting from the linear stability analysis of the inverted pendulum on a cart with delayed linear control, the stability and local Hopf bifurcation induced by the time delay are addressed in Sect. 2. Then in Sect. 3, using the method of multiple scales, the direction of the Hopf bifurcation and the stability of the periodic solutions are determined. Some numerical simulations are performed to illustrate the results of the analysis in Sect. 4. Finally, conclusions are drawn in Sect. 5.

2 Stability and Hopf bifurcation induced by delay

Setting $x_1(t) = \theta(t)$ and $x_2(t) = \dot{\theta}(t)$, Eq. (1) can be written as the following vector form:

$$\begin{cases} \dot{x_1}(t) = x_2(t), \\ \dot{x_2}(t) = \frac{-(3/8)\rho \sin(2x_1(t))x_2^2(t) + \sin x_1(t)}{1-(3/4)\rho\cos^2 x_1(t)} \\ \qquad\quad - \frac{\cos x_1(t)(ax_1(t-\tau)+bx_2(t-\tau))}{1-(3/4)\rho\cos^2 x_1(t)}. \end{cases} \tag{2}$$

The equilibrium $(\hat{x}_1, \hat{x}_2)$ of (2) is determined by $\tan\hat{x}_1 = a\hat{x}_1$ and $\hat{x}_2 = 0$. It is easy to verify that when $a > 1$, the origin $E_0(0,0)$ is an equilibrium together with other two nonzero equilibria $E_1(\hat{x}_{11}, 0)$ and $E_2(\hat{x}_{12}, 0)$; when $a \le 1$, there are two equilibria $E_0(0,0)$ and $E_3(\hat{x}_{13}, 0)$. Here, $\hat{x}_{11}$, $\hat{x}_{12}$, and $\hat{x}_{13}$ are roots of the equation $\tan\hat{x}_1 = a\hat{x}_1$ in the range $[0, 2\pi]$ and satisfy

$$0 < \hat{x}_{11} < \pi/2 < \pi < \hat{x}_{13} < \hat{x}_{12} < 3\pi/2. \tag{3}$$

Linearization of system (2) about the equilibrium $(\hat{x}_1, \hat{x}_2)$ gives

$$\begin{pmatrix} \dot{x_1}(t) \\ \dot{x_2}(t) \end{pmatrix} = \begin{pmatrix} 0 & 1 \\ r_1 & 0 \end{pmatrix} \begin{pmatrix} x_1(t) \\ x_2(t) \end{pmatrix} - \begin{pmatrix} 0 & 0 \\ r_2 a & r_2 b \end{pmatrix} \begin{pmatrix} x_1(t-\tau) \\ x_2(t-\tau) \end{pmatrix}, \tag{4}$$

where

$$r_1 = \frac{\cos\hat{x}_1(1+\tan^2\hat{x}_1)}{1-(3/4)\rho\cos^2\hat{x}_1},$$

$$r_2 = \frac{\cos\hat{x}_1}{1-(3/4)\rho\cos^2\hat{x}_1}.$$

It follows from (3) that

$$r_{1,2} > 0 \quad \text{for } E_0, E_1, \qquad r_{1,2} < 0 \quad \text{for } E_2, E_3. \tag{5}$$

The characteristic equation of system (4) at the equilibrium $(\hat{x}_1, \hat{x}_2)$ is given by

$$\Delta(\tau) = \lambda^2 - r_1 + r_2(b\lambda + a)e^{-\lambda\tau} = 0. \tag{6}$$

Notice whether Eq. (6) has the imaginary roots with zero real part is closely related to the stability and bifurcation of the equilibria. If we assume that $i\omega$ ($\omega > 0$) is a root of Eq. (6), then

$$-\omega^2 - r_1 + r_2(bi\omega + a)(\cos\omega\tau - i\sin\omega\tau) = 0,$$

which is equivalent to

$$\begin{cases} -r_1 - \omega^2 + r_2(b\omega\sin\omega\tau + a\cos\omega\tau) = 0, \\ b\omega\cos\omega\tau - a\sin\omega\tau = 0. \end{cases} \tag{7}$$

From (7), we have

$$\omega^4 + \left(2r_1 - r_2^2b^2\right)\omega^2 + \left(r_1^2 - a^2r_2^2\right) = 0. \tag{8}$$

Set

$$\omega_\pm = \sqrt{\frac{(r_2^2b^2 - 2r_1) \pm \sqrt{4a^2r_2^2 + b^4r_2^4 - 4r_1r_2^2b^2}}{2}}, \tag{9}$$

$$\tau_j^+ = \begin{cases} \frac{1}{\omega_+}\{\arctan(\frac{b}{a}\omega_+) + 2j\pi\}, & r_1, r_2 > 0, \\ \frac{1}{\omega_+}\{\pi + \arctan(\frac{b}{a}\omega_+) + 2j\pi\}, & r_1, r_2 < 0, \end{cases}$$
$$j = 0, 1, 2, \ldots, \tag{10}$$

and

$$\tau_j^- = \frac{1}{\omega_-}\left\{\arctan\left(\frac{b}{a}\omega_-\right) + 2j\pi\right\}, \quad j = 0, 1, 2, \ldots. \tag{11}$$

We first investigate the stability of Hopf bifurcation induced by delay at the zero equilibrium E_0. For the zero equilibrium E_0, we have $r_1 = r_2 = \frac{4}{4-3\rho} > 0$. In this case, (8) becomes

$$\omega^4 + k\big(2 - kb^2\big)\omega^2 + k^2\big(1 - a^2\big) = 0. \tag{12}$$

with $k = \frac{4}{4-3\rho}$. By a simple calculation, one can show that when $0 < a < 1$ and $b < \sqrt{2(1+\sqrt{1-a^2})/k}$, Eq. (12) has no purely imaginary roots; when either $a > 1$ and $b > 0$, or $a = 1$ and $b > \sqrt{2/k}$, or $0 < a < 1$ and $b = \sqrt{2(1+\sqrt{1-a^2})/k}$, Eq. (12) has a pair of purely imaginary roots $\pm i\omega_+$ at τ_j^+; when $0 < a < 1$ and $b > \sqrt{2(1+\sqrt{1-a^2})/k}$, Eq. (12) has a pair of purely imaginary roots $\pm i\omega_+$ (resp. $\pm i\omega_-$) at τ_j^+ (resp. τ_j^-). Denote by

$$\lambda\big(\tau_j^\pm\big) = \mu\big(\tau_j^\pm\big) + i\omega\big(\tau_j^\pm\big), \quad j = 0, 1, 2, \ldots,$$

the root of Eq. (6) satisfying

$$\mu\big(\tau_j^\pm\big) = 0, \qquad \omega\big(\tau_j^\pm\big) = \omega_\pm.$$

From (6) and (7), the derivatives of λ with respect to τ at $\tau_j^\pm$ are

$$\left(\frac{d\lambda}{d\tau}\right)^{-1} = \frac{2e^{\lambda\tau}}{k(b\lambda + a)} + \frac{b}{\lambda(b\lambda + a)} - \frac{\tau}{\lambda}$$

and

$$\mathrm{Re}\left(\left(\frac{d\lambda}{d\tau}\right)\right)\Big|_{\tau=\tau_j^\pm}^{-1} = \pm\frac{\sqrt{4a^2 + b^4k^2 - 4kb^2}}{k(a^2 + b^2\omega_\pm^2)}. \tag{13}$$

Notice the fact that the product of the real parts of $(\frac{d\lambda}{d\tau})$ and $(\frac{d\lambda}{d\tau})^{-1}$ is positive. Then, by (13), we have the following transversality conditions:

$$\frac{d}{d\tau}\mathrm{Re}\,\lambda\big(\tau_j^+\big) > 0, \qquad \frac{d}{d\tau}\mathrm{Re}\,\lambda\big(\tau_j^-\big) < 0.$$

To study the stability of the equilibrium E_0, it is important to determine whether $\tau_0^+ < \tau_0^-$ or not. According to the proof in Appendix A, we have $\tau_0^+ < \tau_0^-$ for the equilibrium E_0.

Clearly, the zero equilibrium E_0 has at least a zero eigenvalue at $a = 1$. In addition, notice that when $\tau = 0$, two roots of Eq. (6) with $r_1 = r_2 = k$ have negative real parts if and only if $a > 1$ and $b > 0$. Therefore, according to the above discussions and Rouchés theorem [21], we have the following results on the distribution of roots of Eq. (6).

Lemma 2.1 *Assuming that $r_1 = r_2 = k$ and $\omega_\pm$ and $\tau_j^\pm$ are defined by (9), (10), and (11), respectively, then for the zero equilibrium E_0, we have the following*:

(i) *When $0 < a < 1$ and $b > 0$, Eq. (6) has at least a root with positive real parts for any $\tau \geq 0$;*

(ii) *When $a > 1$ and $b > 0$, all roots of Eq. (6) have negative real parts for $\tau \in [0, \tau_0^+)$ and Eq. (6) has at least a pair of roots with positive real parts for $\tau > \tau_0^+$;*

(iii) *When $0 < a < 1$ and $b < \sqrt{2(1+\sqrt{1-a^2})/k}$, Eq. (6) has no purely imaginary roots; when $a > 1$ and $b > 0$, or $0 < a < 1$ and $b = \sqrt{2(1+\sqrt{1-a^2})/k}$, Eq. (6) has a pair of purely imaginary roots $\pm i\omega_+$ at τ_j^+; when $0 < a < 1$ and $b > \sqrt{2(1+\sqrt{1-a^2})/k}$, Eq. (6) has a pair of purely imaginary roots $\pm i\omega_+$ (resp. $\pm i\omega_-$) at τ_j^+ (resp. τ_j^-);*

(iv) *When $a = 1$ and $b > \sqrt{2/k}$, Eq. (6) has a zero root $\lambda = 0$ and has a pair of purely imaginary roots $\pm i\omega_+$ at τ_j^+; when $a = 1$ and $b < \sqrt{2/k}$, Eq. (6) has a zero root $\lambda = 0$ and has no other roots on the imaginary axis; when $a = 1$, $b = \sqrt{2/k}$ and $\tau \neq \sqrt{2/k}$, Eq. (6) has a double zero root $\lambda = 0$ and has no other roots on the imaginary axis; when $a = 1$, $b = \tau = \sqrt{2/k}$, Eq. (6) has a triple zero root $\lambda = 0$ and has no other roots on the imaginary axis.*

From Lemma 2.1 and the results regarding the stability and bifurcation of the equilibrium of functional differential equations in [22], we have the following results on the stability of the zero equilibrium of system (2).

Theorem 2.2 *Assuming that* $r_1 = r_2 = k$ *and* $\omega_\pm$ *and* $\tau_j^\pm$ *are defined by* (9), (10), *and* (11), *respectively, then we have the following*:

(i) *When* $0 < a < 1$ *and* $b > 0$, *the zero equilibrium of system* (2) *is unstable for any* $\tau \geq 0$;

(ii) *When* $a > 1$ *and* $b > 0$, *the zero equilibrium of system* (2) *is asymptotically stable for* $\tau \in [0, \tau_0^+)$ *and unstable for* $\tau > \tau_0^+$;

(iii) *When* $a > 1$ *and* $b > 0$, *or* $0 < a < 1$ *and* $b = \sqrt{2(1+\sqrt{1-a^2})}/k$, *system* (2) *undergoes Hopf bifurcations near the zero equilibrium at* τ_j^+; *when* $0 < a < 1$ *and* $b > \sqrt{2(1+\sqrt{1-a^2})}/k$, *system* (2) *undergoes Hopf bifurcations near the zero equilibrium at* $\tau_j^\pm$;

(iv) *When* $a = 1$ *and* $b > \sqrt{2/k}$, *system* (2) *undergoes Hopf bifurcations near the zero equilibrium at* τ_j^+; *when* $a = 1$, $b = \sqrt{2/k}$ *and* $\tau \neq \sqrt{2/k}$, *system* (2) *has a double zero singularity*; *when* $a = 1, b = \tau = \sqrt{2/k}$, *system* (2) *has a triple zero singularity.*

In the following, we analyze the stability and Hopf bifurcations induced by delay for nonzero equilibria. First, it follows from (3), (5), and (6) that when $\tau = 0$, the nonzero equilibria $E_i, i = 1, 2, 3$, have at least one root with positive real part.

By (3) and (5), we have

$$r_1 - ar_2 = \frac{1}{(1-(3/4)\rho\cos^2\hat{x}_1)\cos(\hat{x}_1)} \times \left(1 - \frac{\sin(2\hat{x}_1)}{2\hat{x}_1}\right) \begin{cases} > 0, & \text{for } E_1, \\ < 0, & \text{for } E_2 \text{ and } E_3, \end{cases}$$

and then $r_1^2 - a^2 r_2^2 > 0$ for all nonzero equilibria $E_i, i = 1, 2, 3$. Since $r_1 < 0$ for E_2 and E_3 by (5), we have

$$b^2 r_2^2 - 2r_1 > 0 \quad \text{and} \quad b^4 r_2^4 - 4r_1 r_2^2 b^2 + 4a^2 r_2^2 > 0.$$

So, for nonzero equilibria $E_i, i = 2, 3$, the characteristic equation (6) always has a pair of purely imaginary roots $\pm i\omega_+$ (resp. $\pm i\omega_-$) at τ_j^+ (resp. τ_j^-). Notice that for the equilibrium E_1, $r_{1,2} > 0$ according to (5). Thus, by (10) and (11), it is clear to show that $\tau_0^+ < \tau_0^-$ for E_1 using the same method as for E_0. However, for E_2 and E_3, by (10) and (11), we have

$$\tau_0^+ = \frac{1}{\omega_+}\left\{\pi + \arctan\left(\frac{b}{a}\omega_+\right)\right\},$$

$$\tau_0^- = \frac{1}{\omega_-}\arctan\left(\frac{b}{a}\omega_-\right).$$

Whether $\tau_0^+ > \tau_0^-$ or not is determined by the values of control gains a, b and the relative mass of the pendulum ρ. When some certain values are given, $\tau_0^+ > \tau_0^-$ is satisfied. In Fig. 2, for the nonzero equilibrium E_2, it is clear that the region above the dashed line denoting $\tau_0^+ < \tau_0^-$ while the region below the dashed line denoting $\tau_0^+ > \tau_0^-$. The real line where the nonzero equilibrium appears is just below the dashed line. That is to say for all $1 < a < 4.5$, $\tau_0^+ > \tau_0^-$ is satisfied. In Fig. 3, for the nonzero equilibrium E_3, it is clear that the region in the internal of the dashed line denoting $\tau_0^+ < \tau_0^-$ while the region in the external of the dashed line denoting $\tau_0^+ > \tau_0^-$. The real line where the nonzero equilibrium appears is partly in the external of the dashed line. That is to say for $0.019 < a < 0.097$, $\tau_0^+ < \tau_0^-$ is satisfied.

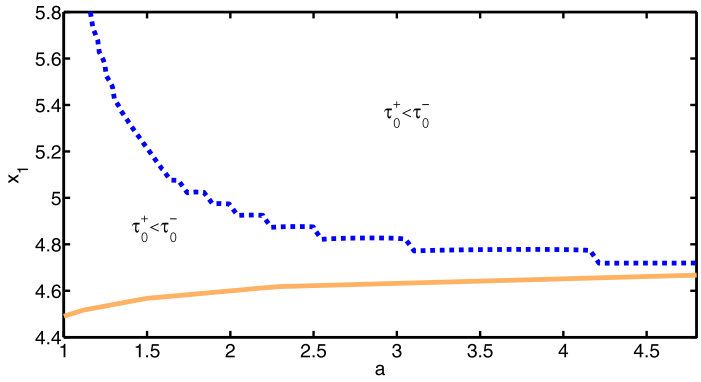

Fig. 2 The relation between critical values of τ_0^+ and τ_0^- for the nonzero equilibrium E_2 when $1 < a < 4.5$. *The dashed line* denotes $\tau_0^+ = \tau_0^-$ when $b = 1$ and $\rho = \frac{2}{3}$; *The real line* denotes $\tan x_1 = a x_1$, where there is the equilibrium E_2 when $b = 1$ and $\rho = \frac{2}{3}$

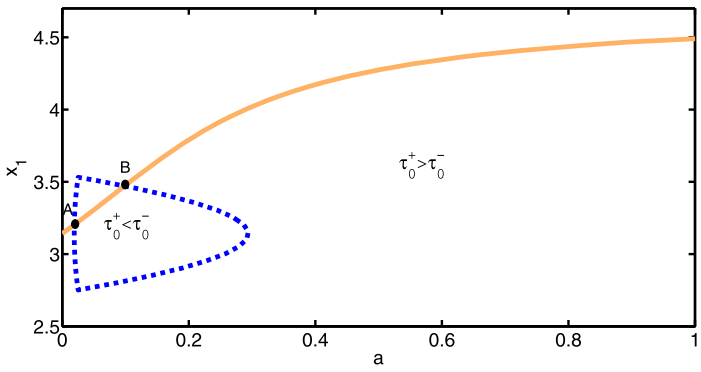

Fig. 3 The relation between critical values of τ_0^+ and τ_0^- for the nonzero equilibrium E_3 when $0 < a < 1$. *The dashed line* denotes $\tau_0^+ = \tau_0^-$ when $b = 1$ and $\rho = \frac{2}{3}$; *The real line* denotes $\tan x_1 = a x_1$, where there is the equilibrium E_3 when $b = 1$ and $\rho = \frac{2}{3}$. The horizontal coordinates of A and B are 0.019 and 0.097

Also, the transversality conditions for the nonzero equilibria hold. That is,

$$\mathrm{Re}\left(\left(\frac{d\lambda}{d\tau}\right)\right)\Big|^{-1}_{\tau=\tau_j^{\pm}} = \pm\frac{\sqrt{4a^2r_2^2 + b^4r_2^2 - 4r_1r_2^2b^2}}{r_2^2(b^2\omega_{\pm}^2 + a^2)}. \tag{14}$$

So, $\frac{d}{d\tau}\mathrm{Re}\,\lambda(\tau_j^+) > 0$, $\frac{d}{d\tau}\mathrm{Re}\,\lambda(\tau_j^-) < 0$. Then we have the following results on the stability and Hopf bifurcations of the nonzero equilibria of system (2).

Theorem 2.3 *Assume that $\omega_{\pm}$ and $\tau_j^{\pm}$ are defined by* (9), (10), *and* (11), *respectively.*

(i) *The nonzero equilibrium E_1 of system* (2) *is unstable for all $\tau \geq 0$.*

(ii) *If $\tau_0^+ < \tau_0^-$, the nonzero equilibria E_2 and E_3 of system* (2) *are unstable for all $\tau \geq 0$, while if $\tau_0^+ > \tau_0^-$, there are positive integers m_p $(p = 1, 2)$ such that the nonzero equilibria E_2 and E_3 of system* (2) *are unstable for*

$$\tau \in [0, \tau_0^-) \cup (\tau_0^+, \tau_1^-) \cup \cdots \cup (\tau_{m_p-1}^+, \tau_{m_p}^-) \cup (\tau_{m_p}^+, +\infty),$$

and stable for

$$\tau \in (\tau_0^-, \tau_0^+) \cup (\tau_1^-, \tau_1^+) \cup \cdots \cup (\tau_{m_p}^-, \tau_{m_p}^+), \quad p = 1, 2,$$

where $p = 1$ and $p = 2$ correspond to E_2 and E_3, respectively.

(iii) *System* (2) *undergoes Hopf bifurcations near the nonzero equilibria E_i $(i = 1, 2, 3)$ at $\tau = \tau_j^{\pm}$.*

3 Direction and stability of Hopf bifurcation

In this section, we apply the method of multiple scales to the nonlinear systems at the zero equilibrium E_0 to obtain the normal form determining the direction of the Hopf bifurcation and the stability of the periodic solutions. This method is useful, for example, in the analysis of systems near a Hopf bifurcation.

Theorems 2.2 and 2.3 show that if $a > 1$ and $b > 0$ or $0 < a < 1$ and $b = \sqrt{2(1 + \sqrt{1 - a^2})/k}$ system (2) undergoes Hopf bifurcation near the zero equilibrium at $\tau_j^{\pm}$. Following the ideas of Nayfeh [23], we derive the explicit formulaes determining the direction and stability of these Hopf bifurcations using the method of multiple scales.

For simplification of notations, we denote the critical value by τ_c and the corresponding purely imaginary roots by $\pm i\omega_c$. Before rescaling the time t, we first add some transformations into the system. Casted into Taylor series truncating the equations at the third-order terms, system (2) reads:

$$\dot{\mathbf{x}} = L\mathbf{x}(t) - R\mathbf{x}(t-\tau) + \mathbf{f}\big[\mathbf{x}(t), \mathbf{x}(t-\tau)\big], \tag{15}$$

where

$$L = \begin{bmatrix} 0 & 1 \\ k & 0 \end{bmatrix}, \qquad R = \begin{bmatrix} 0 & 0 \\ ak & bk \end{bmatrix},$$

$$\mathbf{x}(t) = \begin{bmatrix} x_1(t) \\ x_2(t) \end{bmatrix}, \qquad f = \begin{bmatrix} 0 \\ h_1 \end{bmatrix},$$

in which

$$h_1 = -\left(k^2 - \frac{5}{6}k\right)x_1^3(t) + \left(k^2 - \frac{k}{2}\right) \times \big[ax_1^2(t)x_{1\tau} + bx_1^2(t)x_{2\tau}\big] - (k-1)x_1(t)x_2^2(t)$$

and

$$x_{1\tau} = x_1(t-\tau), \qquad x_{2\tau} = x_2(t-\tau).$$

Rescaling the time by $t \longmapsto t/\tau$, Eqs. (15) become:

$$\dot{\mathbf{x}} = \tau L\mathbf{x}(t) - \tau R\mathbf{x}(t-1) + \tau \mathbf{f}\big[\mathbf{x}(t), \mathbf{x}(t-1)\big]. \quad (16)$$

The linearizing equation of Eq. (16) is

$$L_\tau(\mathbf{x}) = \tau L\mathbf{x}(t) - \tau R\mathbf{x}(t-1). \quad (17)$$

It follows from Lemma 2.1 that at the critical value τ_c the characteristic equation of Eq. (17) has a pair of purely imaginary roots $\pm i\omega_c\tau_c$ and no other roots in the imaginary axis. Theorem 2.3 shows that system (16) undergoes the Hopf bifurcation near the zero equilibrium at $\tau = \tau_c$. The properties of Hopf bifurcation at the critical value τ_c such as direction and stability can be investigated by the so-called normal form. Employing the method of multiple scales as shown in [23] (see Appendix B for details), we have the following normal form truncated the third order associated with the Hopf bifurcation at the critical value τ_c:

$$\frac{dA}{dt} = A\delta\mu_1 + A^2\bar{A}\mu_2, \quad (18)$$

where

$$\mu_1 = \frac{kb\omega_c^2 e^{-i\omega_c\tau_c} - 2k(i\omega_c)(ae^{-i\omega_c\tau_c} - 1)}{k(1-ae^{-i\omega_c\tau_c}) + \omega_c^2(bk\tau_c^2 e^{-i\omega_c\tau_c} - 1) - ak\tau_c^2(i\omega_c)e^{-i\omega_c\tau_c}}$$

and

$$\mu_2 = \frac{(i\omega_c\tau_c)\{-(3k^2 - \frac{5k}{2}) + (k^2 - \frac{k}{2})[2e^{-i\omega_c\tau_c}(a + bi\omega_c) + e^{i\omega_c\tau_c}(a - bi\omega_c] - (k-1)\omega_c^2\}}{k(1-ae^{-i\omega_c\tau_c}) + \omega_c^2(bk\tau_c^2 e^{-i\omega_c\tau_c} - 1) - ak\tau_c^2(i\omega_c)e^{-i\omega_c\tau_c}}.$$

It is convenient for analysis to transform the normal form (18) into polar coordinates. Setting $A = \alpha e^{i\beta}$ where $\alpha = \alpha(t)$ and $\beta = \beta(t)$ then substituting it into Eq. (18) and separating the real and imaginary parts, we can obtain the following real-valued normal form of the bifurcation:

$$\begin{aligned} \frac{d\alpha}{dt} &= \alpha\delta\,\mathrm{Re}\,(\mu_1) + \alpha^3\,\mathrm{Re}\,(\mu_2), \\ \frac{d\beta}{dt} &= \delta\,\mathrm{Im}(\mu_1) + \alpha^2\,\mathrm{Im}(\mu_2). \end{aligned} \quad (19)$$

The equation governing the time variation of β affects the speed of the rotation of the unit angular velocity. But the properties of the Hopf bifurcation like stability and direction is completely determined by the amplitude equation governing the time variation of α. When the values of the parameters are fixed, the signs of $\mathrm{Re}\,(\mu_1)$ and $\mathrm{Re}\,(\mu_2)$ can be obtained. It is well known that the generic Hopf bifurcation corresponds to the situation $\mathrm{Re}\,(\mu_2) \neq 0$, and that the sign of $\mathrm{Re}\,(\mu_1)\,\mathrm{Re}\,(\mu_2)$ determines the direction of the bifurcation and the sign of $\mathrm{Re}\,(\mu_2)$ determines the stability of the nontrivial periodic orbits [25].

Then we have the following results about the direction and stability of Hopf bifurcations at $\tau_j^{\pm}$.

Theorem 3.1 *For* (19), *as parameters* (a, b, ρ, τ) *vary such that*

(i) *When* $\mathrm{Re}\,(\mu_1)\,\mathrm{Re}\,(\mu_2) < 0$, *then the Hopf bifurcation is supercritical type*;
(ii) *When* $\mathrm{Re}\,(\mu_1)\,\mathrm{Re}\,(\mu_2) > 0$, *then the Hopf bifurcation is subcritical type*;
(iii) *If* $\mathrm{Re}\,(\mu_2) < 0$, *the nontrivial periodic solution is stable*; *If* $\mathrm{Re}\,(\mu_2) > 0$, *the nontrivial periodic solution is unstable*.

4 Numerical simulations

To supplement our theoretical work, we consider particular examples and compare the predictions obtained in the previous sections with the numerical simulations by Matlab.

The previous work showed that for the system of the inverted pendulum with delayed control the values of parameters a and b can be marked off to two parameter regions D_1 and D_2. D_1: $a > 1$, $b > 0$, and

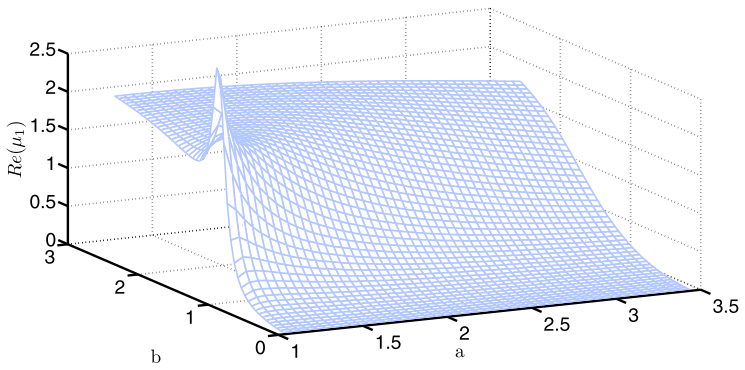

Fig. 4 $\mathrm{Re}(\mu_1)$ as a function of control gains a and b at $\rho = 2/3$

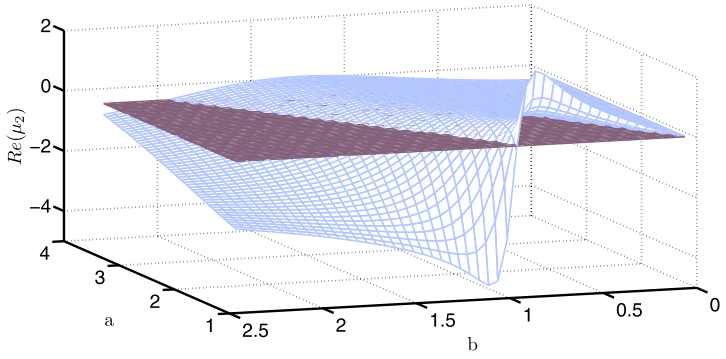

Fig. 5 $\mathrm{Re}(\mu_2)$ as a function of control gains a and b at $\rho = 2/3$

D_2: $0 < a < 1$, $b > 0$. When a and b belong to D_1, there are three equilibria E_0, E_1 and E_2. When it comes to D_2, there are two equilibria E_0 and E_3. In the following subsections we consider the different regions orderly to perform the numerical computations.

4.1 D_1: $a > 1, b > 0$

According to Theorem 3.1, the direction and stability of Hopf bifurcations are determined by the signs of $\mathrm{Re}(\mu_1)\,\mathrm{Re}(\mu_2)$ and $\mathrm{Re}(\mu_2)$, respectively. We can see from Fig. 4 that $\mathrm{Re}(\mu_1) > 0$. Thus, the direction and stability of Hopf bifurcations are completely determined by the sign of $\mathrm{Re}(\mu_2)$. Figure 5 shows the effect of the control gains a and b on $\mathrm{Re}(\mu_2)$. In the $a - b$ plane, there are two regions: one corresponds to $\mathrm{Re}(\mu_2) < 0$, which implies the occurrence of the supercritical Hopf bifurcation, and the other corresponds to $\mathrm{Re}(\mu_2) < 0$, which implies the occurrence of the subcritical Hopf bifurcation. In the case of supercritical Hopf bifurcation, there exists a stable periodic orbit near the zero equilibrium for sufficiently small $\mu > 0$. In the case of subcritical Hopf bifurcation, the Hopf bifurcation occurs for sufficiently small $\mu < 0$ and the bifurcating periodic orbit is unstable. In the following numerical simulations, we are interested in the supercritical Hopf bifurcations. Taking $a = 1.55$, $b = 1$, and $\rho = 2/3$, then we have

$$E_0 = (0, 0), \qquad E_1 \doteq (1, 0), \qquad E_2 \doteq (4.5722, 0).$$

According to Theorem 2.3, E_1 is unstable for all $\tau \geq 0$. For the zero equilibrium E_0, when $\tau = 0$ E_0 is stable. As τ varies, according to Theorem 2.1 the zero equilibrium E_0 changes from stability to instability due to the Hopf bifurcation at $\tau = \tau_0^+$ near E_0. By (10), we have the critical value $\tau_0^+ \doteq 0.5080$. Then, in terms of Figs. 4 and 5, we have

$$\mathrm{Re}(\mu_1) > 0, \qquad \mathrm{Re}(\mu_2) < 0,$$

which implies that system (2) undergoes a supercritical Hopf bifurcation at τ_0^+. When we take $\tau = 0.47 < \tau_0^+$, the equilibrium is stable, as shown in Fig. 6. Comparatively, when we take $\tau = 0.52 > \tau_0^+$, the zero equilibrium is unstable with a stable periodic solution (Fig. 7). In addition, we make it clear that all

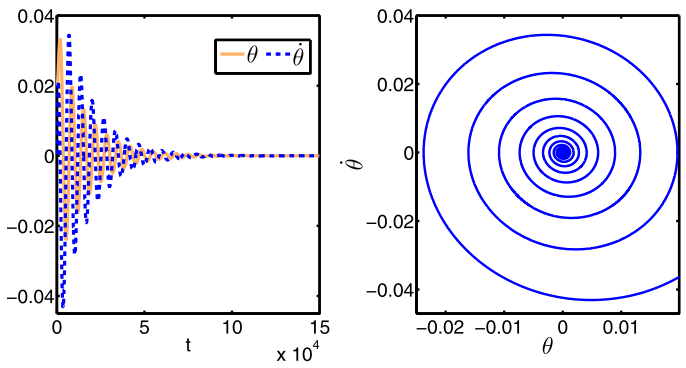

Fig. 6 When $\tau = 0.47 < \tau_0^+$, $a = 1.55$, $b = 1$, $\rho = \frac{2}{3}$, there is no periodic solution bifurcating from E_0 and the zero equilibrium E_0 is stable. The initial value is $(0.2, 0.05)$

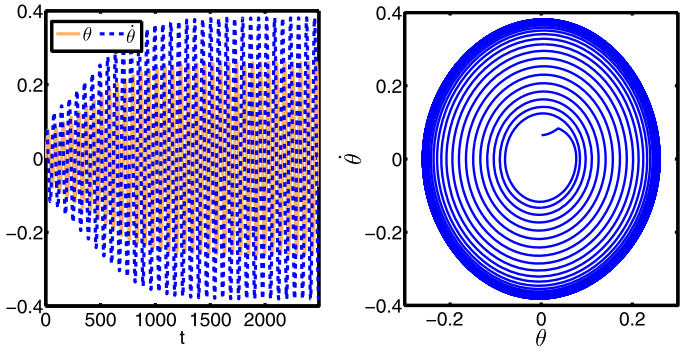

Fig. 7 When $\tau = 0.52 > \tau_0^+$, $a = 1.55$, $b = 1$, $\rho = \frac{2}{3}$, the periodic solution bifurcating from E_0 is stable. The initial value is $(0.005, 0.005)$

the results above are local. That is, they are available only for a sufficient small neighborhood of the critical time delay.

As for the nonzero equilibrium E_2, it follows from Eqs. (10) and (11) that

$$\tau_0^+ \doteq 1.5169, \qquad \tau_0^- \doteq 0.3967.$$

According to Theorem 2, there are stability switches for $\tau \geq 0$. We can calculate more values of the critical delays $\tau_j^{\pm}$ and find out that

$$\begin{aligned}\tau_0^- < \tau_0^+ < \tau_1^- < \tau_1^+ < \tau_2^- < \tau_2^+ \cdots \\ < \tau_6^- < \tau_6^+ < \tau_7^- < \tau_7^+ < \tau_8^+ < \tau_8^-.\end{aligned}$$

Theorem 2.3 implies that there are 8 switches from instability to stability back to instability, E_2 is unstable for

$$\tau \in \left[0, \tau_0^-\right) \cup \left(\tau_0^+, \tau_1^-\right) \cup \cdots \cup \left(\tau_6^+, \tau_7^-\right) \cup \left(\tau_7^+, +\infty\right),$$

and stable for

$$\tau \in \left[\tau_0^-, \tau_0^+\right) \cup \left(\tau_1^-, \tau_1^+\right) \cup \cdots \cup \left(\tau_7^-, \tau_7^+\right).$$

So, the nonzero equilibrium E_2 is unstable for $\tau \in [0, \tau_0^-)$ and stable for $\tau \in (\tau_0^-, \tau_0^+)$. Here, we take $\tau = 0.396$ and $\tau = 0.9$ for the numerical simulations (Fig. 8).

4.2 D_2: $0 < a < 1$, $b > 0$

According to Theorem 2.1, when a and b belong to D_2 and for all $\tau \geq 0$, E_0 is unstable.

As for the nonzero equilibrium E_3, when we take the parameters $a = 0.2305$, $b = 1$, and $\rho = 2/3$, for the nonzero equilibrium E_3 ($E_3 \doteq (3.87, 0)$), it follows from Eq. (11):

$$\tau_0^+ \doteq 2.3221, \qquad \tau_0^- \doteq 1.4272,$$
$$\tau_1^+ \doteq 5.4964, \qquad \tau_1^- \doteq 8.1799.$$

Hence, $\tau_0^+ > \tau_0^-$ is satisfied and

$$\tau_0^- < \tau_0^+ < \tau_1^+ < \tau_1^-.$$

Theorem 2.3 implies that there is only 1 switch from instability to stability back to instability, the nonzero equilibrium E_3 is stable for $\tau \in (\tau_0^-, \tau_0^+)$ (Fig. 9) or $\tau > \tau_0^+$, and unstable for $\tau \in [0, \tau_0^-)$ (Fig. 9).

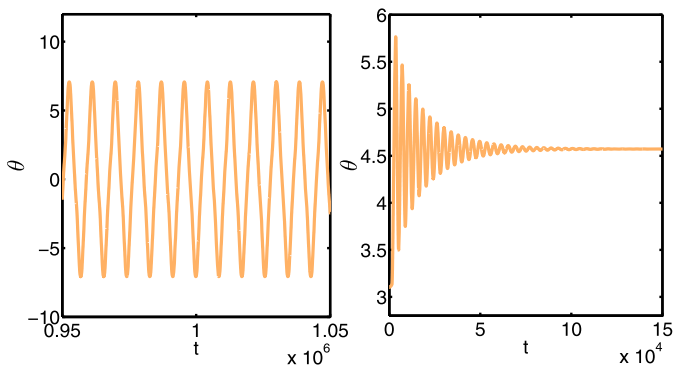

Fig. 8 *The left figure*: When $\tau \in [0, \tau_0^-)$, the equilibrium E_2 is unstable. Here, $\tau = 0.396$, $a = 1.55$, $b = 1$, $\rho = \frac{2}{3}$. The initial values is $(4.2, 0)$; *The right figure*: When $\tau \in [\tau_0^-, \tau_0^+)$, the equilibrium E_2 is stable. Here, $\tau = 0.9$, $a = 1.55$, $b = 1$, $\rho = \frac{2}{3}$. The initial values is $(3.1, 0)$

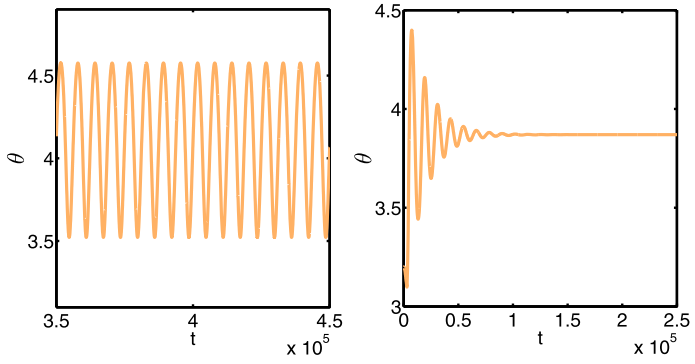

Fig. 9 *The left figure*: When $\tau \in [0, \tau_0^-)$, the equilibrium E_3 is unstable. Here, $\tau = 1.37$, $a = 0.2305$, $b = 1$, $\rho = \frac{2}{3}$. The initial values is $(3.82, 0.005)$; *The right figure*: When $\tau \in [\tau_0^-, \tau_0^+)$, the equilibrium E_3 is stable. Here, $\tau = 1.77$, $a = 0.2305$, $b = 1$, $\rho = \frac{2}{3}$. The initial values is $(3.82, 0.005)$

5 Conclusion

In this paper, the model for an inverted pendulum on a cart with delayed control in the horizontal direction has been studied. We investigated the stability of the zero equilibrium together with the nonzero ones. The $a - b$ parameter plane has been marked off to different regions through the linear stability analysis. The results of the stability and Hopf bifurcation analysis showed that when certain parameter values of a, b and ρ are chosen and the time delay τ varies the model achieves stability of the inverted pendulum in the upright position and also another one or two position(s). While in other parameter regions, the robustness induced by the time delay can occur. Even for the nonzero equilibria E_2 and E_3, there exist stability switches from instability to stability back to instability at some fixed values as τ varies. Using the control gains a and b, the relative mass of the pendulum ρ as the initial systemic parameters and the time delay τ as perturbation parameter, we studied the direction of the Hopf bifurcation and the stability of the periodic solutions of the zero equilibrium E_0 applying the method of multiple scales. The normal form derived reflects both supercritical or subcritical type of Hopf bifurcation can emerge for certain parameter values.

Our numerical simulations in Sect. 4 are parallel with the theoretical conclusions for the stability and Hopf bifurcation induced by the time delay. For certain parameter values, there is a supercritical Hopf bifurcation with stable periodic solutions of the zero equilibrium E_0. Numerical simulation implied that for the nonzero equilibrium there are larger amplitude periodic solutions and more complicated dynamics occur. In fact, except for Hopf bifurcation, there are codimension 2 bifurcations such as double Hopf bifurcations and Hopf-zero singularities in this inverted pendulum system with delayed feedback control, leading to more complex dynamics. We will leave the investigation of these codimension 2 bifurcations in the future.

Acknowledgements The authors highly appreciate the anonymous reviewers for providing valuable suggestions which helped us to improve the manuscript. The research are supported by the National Natural Science of China (No. 11101076), the Shanghai Committee of Science and Technology (No.

11ZR1400200), the Scientific Research Foundation for the Returned Overseas Chinese Scholars, the Fundamental Research Funds for the Central Universities, and the Program for New Century Excellent Talents in University (NCET-11-0385).

Appendix A: Proof for $\tau_0^+ < \tau_0^-$

Since $r_1 = r_2 = k > 0$ for the zero equilibrium, it follows from (10) and (11) that

$$\tau_0^+ = \frac{1}{\omega_+} \arctan\left(\frac{b}{a}\omega_+\right),$$

$$\tau_0^- = \frac{1}{\omega_-} \arctan\left(\frac{b}{a}\omega_-\right).$$

Define a function f of x as follows:

$$f(x) = \frac{1}{x} \arctan\left(\frac{b}{a}x\right), \quad x > 0,$$

and then we have

$$f'(x) = \frac{\frac{b}{a}x - \arctan(\frac{b}{a}x)(1+\frac{b^2}{a^2}x^2)}{x^2(1+\frac{b^2}{a^2}x^2)}.$$

Denote the denominator of the right hand of $f'(x)$ by

$$g(x) = \frac{b}{a}x - \arctan\left(\frac{b}{a}x\right)\left(1+\frac{b^2}{a^2}x^2\right).$$

Then we have

$$g(0) = 0, \quad g'(x) = -\arctan\left(\frac{b}{a}x\right)\frac{2b^2}{a^2}x < 0,$$

which implies that $g(x) < 0$ for $x \in (0, \infty)$. Thus, $f(x)$ is a monotone decreasing function on $x \in (0, \infty)$. This, together with $\omega_+ > \omega_-$, means that $\tau_0^+ < \tau_0^-$.

Appendix B: Derivation of normal form (19)

Let $\mathbf{p}$ be the eigenvector of L_τ corresponding to the eigenvalue $i\omega_c\tau_c$, and let $\mathbf{q}$ be the normalized eigenvector of the adjoint operator of L_τ corresponding to the eigenvalue $-i\omega_c\tau_c$ with the inner product

$$\langle \mathbf{q}, \mathbf{p}\rangle = \sum_{i=1}^{2} \bar{q}_i p_i = 1.$$

By simple calculations, we have

$$\mathbf{p} = (p_1, p_2)^T, \qquad \mathbf{q} = (q_1, q_2)^T. \tag{20}$$

Where

$$p_1 = 1, \qquad p_2 = i\omega_c, \qquad q_1 = \frac{k(ae^{i\omega_c\tau_c} - 1)}{2\omega_c^2 + kb(i\omega_c)e^{i\omega_c\tau_c}},$$

$$q_2 = \frac{i\omega_c}{2\omega_c^2 + kb(i\omega_c)e^{i\omega_c\tau_c}}.$$

We are now in a position to apply the method of multiple scales to investigate the properties of Hopf bifurcation at the critical value τ_c. Because the nonlinearity has no second order terms, we seek a uniform second-order approximate solution of Eq. (16) in power of $\epsilon^{1/2}$. Since the periodic solution of Hopf bifurcation is a small amplitude periodic solution near the zero equilibrium, we assume that a series solution of Eq. (16) has the following form:

$$\mathbf{x}(t;\epsilon) = \epsilon^{1/2}\mathbf{x}_1(T_0, T_1) + \epsilon^{3/2}\mathbf{x}_2(T_0, T_1) + \cdots, \tag{21}$$

where $T_0 = t$, $T_1 = \epsilon t$, and ϵ is a nondimensional book-keeping parameter. Notice that the secular terms first appear at $O(\epsilon^{3/2})$. So, it is sufficient for the time scale of the second argument to be taken as the form of $T_1 = \epsilon t$. By the chain rule, we would like to introduce the following differential operator:

$$\frac{d}{dt} = \frac{\alpha}{dT_0} + \epsilon\frac{\alpha}{\alpha T_1} = D_0 + \epsilon D_1. \tag{22}$$

In terms of the scales T_0 and T_1, with the expansion for small ϵ the delayed variable $\mathbf{x}(t-1)$ can be expressed as

$$\mathbf{x}(t-1;\epsilon) = \epsilon^{1/2}\mathbf{x}_1(T_0 - 1, T_1) + \epsilon^{3/2}\mathbf{x}_2(T_0 - 1, T_1) - \epsilon^{3/2}\tau D_1\mathbf{x}_1(T_0 - 1, T_1) + \cdots. \tag{23}$$

Next, we introduce the detuning parameter δ to describe the nearness of τ to the critical value τ_c defined by

$$\tau = \tau_c + \epsilon\delta. \tag{24}$$

Substituting Eqs. (21)–(24) into Eq. (16) leads to the following perturbation equations, written up to the $\epsilon^{3/2}$ order:

$$\epsilon^{1/2}: \quad D_0\mathbf{x}_1(T_0, T_1) - L\tau_c\mathbf{x}_1(T_0, T_1) + R\tau_c\mathbf{x}_1(T_0 - 1, T_1) = 0, \tag{25}$$

$$\begin{aligned}\epsilon^{3/2}: \quad & D_0\mathbf{x}_2(T_0,T_1) - L\tau_c\mathbf{x}_2(T_0,T_1) \\ & + R\tau_c\mathbf{x}_2(T_0-1,T_1) \\ = & -D_1\mathbf{x}_1(T_0,T_1) + \delta L\mathbf{x}_1(T_0,T_1) \\ & + \tau_c^2 R D_1\mathbf{x}_1(T_0-1,T_1) \\ & - \delta R\mathbf{x}_1(T_0-1,T_1) \\ & + \tau_c\mathbf{f}\big[\mathbf{x}_1(t),\mathbf{x}_1(t-1)\big]. \end{aligned} \tag{26}$$

Equation (25) is the linear homogeneous equation and has a pair of simple imaginary roots $\pm i\omega_c\tau_c$ and all other eigenvalues have negative real parts. The general solution is therefore given by

$$\mathbf{x}_1(T_0,T_1) = A(T_1)\mathbf{p}e^{i\omega_c\tau_c T_0} + \bar{A}(T_1)\bar{\mathbf{p}}e^{-i\omega_c\tau_c T_0}, \tag{27}$$

where the vector is defined by (20).

Due to the characteristic equation, we can obtain that ω_c and τ_c satisfy the equation

$$\omega_c^2 + k = kb(i\omega_c)e^{-i\omega_c\tau_c} + kae^{-i\omega_c\tau_c}. \tag{28}$$

Substituting (27) into Eq. (26) yields

$$\begin{aligned} & D_0\mathbf{x}_2(T_0,T_1) - L\tau_c\mathbf{x}_2(T_0,T_1) + R\tau_c\mathbf{x}_2(T_0-1,T_1) \\ & = \big\{\big[-I + \tau_c^2\,\mathrm{Re}^{-i\omega_c\tau_c}\big]\mathbf{p}A' \\ & \quad + \big[\delta L - \delta\,\mathrm{Re}^{-i\omega_c\tau_c}\big]\mathbf{p}A + \tau_c f_* A^2\bar{A}\big\}e^{i\omega_c\tau_c T_0} \\ & \quad + \text{c.c} + \text{NST}, \end{aligned} \tag{29}$$

where

$$f_* = \begin{bmatrix} 0 \\ h_2 \end{bmatrix}. \tag{30}$$

In which

$$\begin{aligned} h_2 = & -\left(3k^2 - \frac{5k}{2}\right) + \left(k^2 - \frac{k}{2}\right) \\ & \times \big[2e^{-i\omega_c\tau_c}(a+bp_2) + e^{i\omega_c\tau_c}(a+b\bar{p}_2)\big] \\ & - (k-1)\big(2p_2\bar{p}_2 + p_2^2\big), \end{aligned}$$

where c.c and NST stand for the complex conjugate of the preceding terms and terms that do not produce secular terms.

Equation (29) is the linear nonhomogeneous equation for $\mathbf{x}_2$. We seek its particular solution in the form

$$\mathbf{x}_2(T_0,T_1) = \phi(T_1)e^{i\omega_c\tau_c T_0}. \tag{31}$$

Substituting Eq. (31) into Eq. (29) and deleting $e^{i\omega_c\tau_c T_0}$, we have

$$\begin{aligned} & \big[i\omega_c\tau_c I - \tau_c L + \tau_c R e^{-i\omega_c\tau_c}\big]\phi \\ & = \big[-I + \tau_c^2\,\mathrm{Re}^{-i\omega_c\tau_c}\big]\mathbf{p}A' + \big[\delta L - \delta\,\mathrm{Re}^{-i\omega_c\tau_c}\big]\mathbf{p}A \\ & \quad + \tau_c f_* A^2\bar{A}, \end{aligned} \tag{32}$$

where I is the 3×3 identity matrix.

It is clear that $\det(L_\tau - i\omega_c\tau_c I) = 0$ since $i\omega_c\tau_c$ is the eigenvalue of L_τ. So, we have a slight problem solving Eq. (32). This difficulty is easy to overcome following the idea of Kuznetsov [24]. In fact, let T^{su} be the real eigenspace corresponding to all eigenvalues of L_τ other than $\pm i\omega_c\tau_c$. We have that $y \in T^{su}$ if and only if $< \mathbf{q}, y >= 0$. From [24], the restriction of the linear formation corresponding to $(L_\tau - i\omega_c\tau_c I)$ to its invariant subspace T^{su} is invertible. That is to say if the right-hand side of Eq. (32) belongs to invariant subspace T^{su} and then Eq. (32) has a unique solution $\phi \in T^{su}$ by solving so-called *bordered system*. Thus, the nonhomogeneous Eq. (32) has solutions provided that the right-hand side of Eq. (32) be orthogonal to every solution of the adjoint homogeneous problem. Letting the inner product of the right-hand side of Eq. (32) with $\mathbf{q}$ be zero yields the solvability condition (18).

References

1. Eltohamy, K.G., Kuo, C.Y.: Real time stabilisation of a triple link inverted pendulum using single control input. IEE Proc., Control Theory Appl. **144**(5), 498–504 (1997)
2. Bugeja, M.: Nonlinear Swing-up and Stabilizing Control of an Inverted Pendulum System vol. 2, pp. 437–441. IEEE Press, New York (2003)
3. Medrano-Creda, G.A.: Robust computer control of an inverted pendulum. IEEE Control Syst. Mag. **19**(3), 58–67 (1999)
4. Van der Linden, G.W., Lambrechts, P.F.: H_∞ control of an experimental inverted pendulum with dry friction. IEEE Control Syst. Mag. **13**(4), 44–50 (1993)
5. Yoshida, K.: Swing-up control of an inverted pendulum by energybased methods. In: Proceedings of the 1999 American Control Conference, vol. 6, pp. 4045–4047 (1999)
6. Enikov, E., Stépán, G.: Stabilizing an inverted pendulum-alternatives and limitations. Mech. Eng. **38**, 19–26 (1994)
7. Wollacott, M.H., von Hosten, C., Rósblad, B.: Relation between muscle response onset and body segmental movements during postural perturbations in humans. Exp. Brain Res. **72**, 593–604 (1998)
8. Campell, S.A., Crawford, S., Morris, K.A.: Time delay and feedback control of an inverted pendulum with stick slip friction. In: 6th International Conference on Multibody Systems, Nonlinear Dynamics and Control, vol. 5, pp. 749–756 (2007)

9. Sieber, J., Krauskopf, B.: Bifurcation analysis of an inverted pendulum with delayed feedback control near a triple-zero eigenvalue singularity. Nonlinearity **17**(1), 88–104 (2004)
10. Sieber, J., Krauskopf, B.: Complex balancing motions of an inverted pendulum subject to delayed feedback control. Physica D **197**, 332–345 (2004)
11. Ibrahim, R.: Excitation-induced stability and phase transition. J. Vib. Control **12**(10), 1093–1170 (2006)
12. Kollá, L.E., Stépán, G., Hogan, S.: Sampling delay and backlash in the balancing systems. Mech. Eng. **44**, 77–84 (2000)
13. Kollár, L.E., Stépán, G.: Digital controlling of piecewise linear systems. Digital controlling of piecewise linear systems. In: Proceedings of the 2nd International Conference on Control of Oscillations and Chaos (Cat. No. 00TH8521). IEEE, vol. 2, pp. 327–330 (2000)
14. Stépán, G., Kollá, L.E.: Balancing with reflex delay. Math. Comput. Model. **31**, 199–205 (2000)
15. Atay, F.M.: Balancing the inverted pendulum using position feedback. Appl. Math. Lett. **12**, 51–56 (1999)
16. Landry, M., Campbell, S.A., Morris, K., Aguilar, C.O.: Dynamics of an inverted pendulum with delayed feedback control. SIAM J. Appl. Dyn. Syst. **4**, 333–351 (2005)
17. Milton, J., Cabrera, J.L., Ohira, T., Tajima, S., Tonosaki, S., Christian, W.E., Campbell, S.A.: The time-delayed inverted pendulum: implications for human balance control. Chaos **19**, 026110 (2009)
18. Campbell, S.A., Crawford, S., Morris, K.: Friction and the inverted stabilization problem. SIAM J. Appl. Dyn. Syst. **130**, 054502 (2008)
19. Cabrera, J.L., Milton, J.G.: On–Off intermittency in a human balancing task. Phys. Rev. Lett. **89**, 158702 (2002)
20. Sieber, J., Krauskopf, B.: Extending the permissible control loop latency for the controlled inverted pendulum. Dyn. Syst. **20**, 189–199 (2005)
21. Dieudonné, J.: Foundations of Modern Analysis. Academic Press, New York (1960)
22. Hale, J.K., Lunel, S.M.V.: Introduction to Functional Differential Equations. Springer, New York (1993)
23. Nayfeh, A.H.: Order reduction of retarded nonlinear systems-the method of multiple scales versus center-manifold reduction. Nonlinear Dyn. **51**, 482–500 (2008)
24. Kuznetsov, Y.A.: Elements of Applied Bifurcation Theory. Springer, Berlin (1998)
25. Chow, S.N., Hale, J.K.: Methods of Bifurcation Theory. Springer, New York (1982)